

Article

XPS and AFM Investigations of Ti-Al-N Coatings Fabricated Using DC Magnetron Sputtering at Various Nitrogen Flow Rates and Deposition Temperatures

Aleksei Obrosov ^{1,*}, Roman Gulyaev ², Markus Ratzke ³, Alex A. Volinsky ⁴, Sebastian Bolz ¹, Muhammad Naveed ¹ and Sabine Weiß ¹

¹ Chair of Physical Metallurgy and Materials Technology, Brandenburg Technical University, 03046 Cottbus, Germany; sebastian.bolz@b-tu.de (S.B.); muhammad.naveed@b-tu.de (M.N.); sabine.weiss@b-tu.de (S.W.)

² Boreskov Institute of Catalysis SB RAS, 630090 Novosibirsk, Russia; gulyaev@catalysis.ru

³ Chair of Experimental Physics II/Materials Science, Brandenburg Technical University, 03046 Cottbus, Germany; markus.ratzke@b-tu.de

⁴ Department of Mechanical Engineering, University of South Florida, Tampa, FL 33620, USA; volinsky@usf.edu

* Correspondence: aleksei.obrosov@b-tu.de; Tel.: +49-355-694-251

Academic Editor: Hugo F. Lopez

Received: 15 November 2016; Accepted: 3 February 2017; Published: 10 February 2017

Abstract: Ti-Al-N coatings were deposited by direct current magnetron sputtering (DCMS) onto IN 718 at different nitrogen flow rates and deposition temperatures. The coatings' properties were characterized using atomic force microscopy (AFM), X-ray photoelectron spectroscopy (XPS) as well as nanoindentation. It was found that higher deposition temperature leads to higher surface roughness and nitrogen flux influences the shape of grains. According to XPS, the bonding structure of all coatings exhibited the (Ti,Al)N phase. Mechanical properties depend on the Al content within the films. The coating with the best mechanical properties (deposited at 500 °C and 20 standard cubic centimeters per minute (scm)) was further deposited onto tungsten carbide (WC) cutting tools for cylindrical turning experiments. A quasi-constant flank wear was observed until a machining volume of 23,500 mm³.

Keywords: Ti-Al-N coatings; DC magnetron sputtering; XPS; AFM; nitrogen flow rate; surface morphology

1. Introduction

Ti-Al-N coatings have been successfully developed since the 1980s because they could significantly increase lifetime of high speed machining tools in comparison with conventional TiN coatings [1,2]. Ti-Al-N films with cubic NaCl (c) structure, where Al substitutes Ti in the TiN based structure, are widely used in the tool industry due to their very good oxidation resistance [3]. Furthermore, these films exhibit high hardness, good wear resistance and age-hardening abilities, along with lower thermal expansion, lower thermal conductivity and enhanced erosion resistance compared to TiN [4–6].

Properties of Ti-Al-N are strongly dependent on their chemical composition [7,8]. The Al content in Ti-Al-N coatings overcomes the oxidation problems, but a superficial Al₂O₃ layer formed at high temperature [9–11]. Al₂O₃ curbs oxygen diffusion and oxidative wear. Depending on the elemental and phase composition, hardness of these coatings can range from 20 to 35 GPa [12–14].

A number of different coating techniques, such as arc ion plating [15], arc evaporation [12,16], radio frequency magnetron sputtering [17], and chemical vapor deposition [4] have been used. However,

magnetron sputtering [18,19] is a widely used method for depositing Ti-Al-N coatings due to control of the film thickness, structure and properties. However, the influence of nitrogen flow rate at different deposition temperatures on the chemical bonding structure and surface morphology of the coatings is hardly discussed.

In the present investigation, Ti-Al-N films were deposited at 200 °C and 500 °C with different nitrogen flow rates on Inconel 718 via the reactive sputter deposition process. The aim of this work is to analyze the influence of deposition temperature and nitrogen flow rate on chemical composition, surface morphology and mechanical properties by X-ray photoelectron spectroscopy (XPS), atomic force microscopy (AFM) and nanoindentation. Furthermore, the coating with the best properties was deposited onto a tungsten carbide (WC) cutting tool for an application oriented turning test.

2. Experimental Section

Ti-Al-N films were deposited in an industrial coater CemeCon 800/9 from CemeCon AG (Würselen, Germany) onto Inconel 718 substrates and WC cutting tools for a cylindrical turning experiment. Prior to coating, the substrates were mirror polished, ultrasonic cleaned and dried. A composite TiAl target (Ti-50%, Al-50%) with a size of 88 mm × 500 mm from PLANSEE AG (Reutte, Austria) was used for the experiments in a reactive sputtering mode. The initial coating process consists of an argon ion etching process, which was performed for 30 min at a substrate MF bias of 650 V and a pressure of 350 MPa. Later, a cathode power of 4 kW with an argon pressure of 600 MPa at a substrate bias of 60 V was used for the deposition process. Moreover, a deposition time of 30 min in a static mode was opted to ensure high deposition rates. Further information about deposition temperature and nitrogen flow rates in standard cubic centimeters per minute (sccm) are given in Table 1.

Table 1. Deposition parameters of Ti-Al-N coatings at various process parameters.

Deposition Temperature (°C)	N ₂ Flow Rate (sccm)
200	20, 40, 60
500	20, 40, 60

A scanning electron microscope (SEM) and wavelength dispersive spectroscopy (WDS) from TESCAN MIRA II (Brno, Czech Republic) were used for characterizing coating growth and elemental analysis.

An ES300 KRATOS spectrometer (Kratos Analytical, Manchester, UK) was used for XPS studies. The surface of the samples was cleaned by washing several times in pure ethanol, dried and placed into a spectrometer. Photoelectron spectra were acquired after evacuation to ultra-high vacuum (UHV, 5×10^{-9} mbar). The electron analyzer was calibrated against Au4f7/2 (84 eV) and Cu2p2/3 (932.7 eV) photoelectron line positions obtained from cleaned gold and copper metallic surfaces. Non-monochromatic Mg K α radiation was used for analysis without calibration because of the conductivity of the samples. Additionally, all samples were characterized after evacuation to UHV and an Ar⁺ ion etching beam at 1 keV and 20 mA was used for 30 min to remove the topmost contaminated layers. Mathematical spectra processing was performed using XPS-Calc software (Boreskov Institute of catalysis, Novosibirsk, Russia), described in [20].

Surface images and roughness of the films were obtained by AFM (“Smena” microscope by NT-MDT, Zelenograd, Russia) operating in the contact mode. Silicon cantilever NSG 11 Pt (NT-MDT, Zelenograd, Russia) with a tip radius of 10 nm was used in this work. The hardness of the coatings was measured by UNAT nanoindenter with a Berkovich indenter (ASMEC GmbH, Radeberg, Germany). Hardness and elastic modulus of the coatings were calculated by analyzing the load-displacement curves using the Oliver Pharr method [21] at a load of 10 mN. The penetration depth did not reach more than one-tenth of the coating thickness to avoid effects from the substrate [22]. An average value of 15–20 measurements was calculated for each film. A cylindrical turning experiment was

carried out under wet cutting conditions on the computer numeric control (CNC) slant bed lathe type VDF 180 C U (Oerlikon-Boehringer, Göppingen, Germany). The turning test of the WC cutting tool with the geometry of CNMN 120408 according to ISO 1832 was carried out with a cutting speed of $v_c = 100$ m/min, a feed of $f = 0.1$ mm/rev and a depth of cut of $a_p = 0.5$ mm. A cutting edge radius of approximately $r_\beta = 35$ μm was determined for the cutting tool. In this work, cold work tool steel, type X210CrW12, was used for the turning test. For the examination of the wear form, the flank wear VB was measured until reaching the defined tool life criterion $VB_{\text{max}} = 0.5$ mm. The clearance angle was $\alpha_{\text{eff}} = 10^\circ$, and the rake angle was $\gamma_{\text{eff}} = -10^\circ$ [23,24].

3. Results and Discussion

3.1. SEM and AFM

A typical cross-sectional SEM image of the Ti-Al-N coating on IN 718 is shown in Figure 1. The dense columnar microstructure of the coating can be attributed to ion bombardment during deposition.

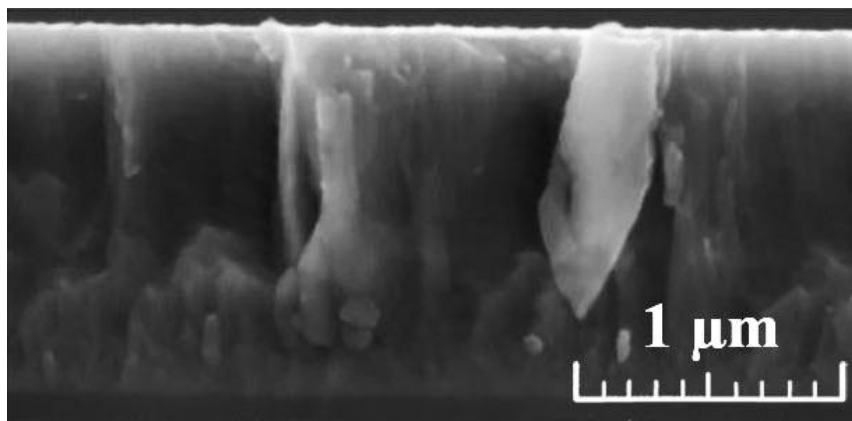


Figure 1. Cross-sectional SEM of the Ti-Al-N film.

WDS analysis of the deposited Ti-Al-N coatings can be seen in Table 2. Al content first increases and then decreases to 44.78 at. % with rising nitrogen flow rate at 200 °C. In contrast, a decrease of Al content from 43.76 to 36.08 at. % takes place with rising nitrogen flow rate at 500 °C.

Table 2. Chemical composition of the Ti-Al-N coatings by means of WDS analysis.

Temperature (°C)	Nitrogen Flow Rate (sccm)	Ti (at. %)	Al (at. %)
200	20	51.46	48.54
	40	48.47	51.53
	60	55.22	44.78
500	20	56.24	43.76
	40	58.04	41.96
	60	51.92	36.09

The surface morphology of the coated IN 718 samples examined by AFM is presented in Figure 2. Topography of the coatings produced at different conditions shows a significant difference in surface roughness and typical surface features. The main characteristics of the films, such as thickness and surface roughness (root-mean-square, RMS) are listed in Table 3.

Coatings fabricated at 200 °C exhibit a densely packed structure consisting of well-separated grains with apparently spherical form (Figure 2a–c). With an increasing nitrogen flow rate, a decrease in roughness (root-mean-square values) was measured. This decrease is mainly attributed to a denser

packing of surface features. According to Shum et al. [25], the Al content plays an important role in smoothing of the film, especially in the range between 20 and 50 at. % due to more nuclei.

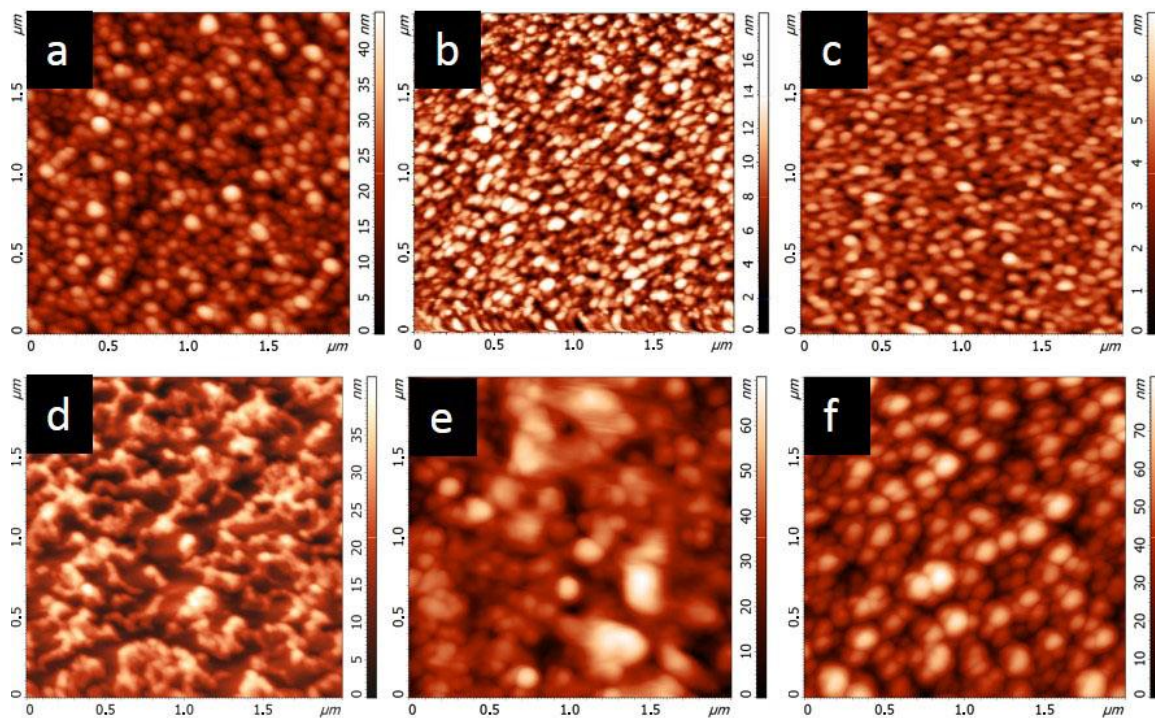


Figure 2. AFM images of Ti-Al-N films (a) 200 °C, 20 sccm; (b) 200 °C, 40 sccm; (c) 200 °C, 60 sccm; (d) 500 °C, 20 sccm; (e) 500 °C, 40 sccm and (f) 500 °C, 60 sccm.

Table 3. Influence of temperature and nitrogen flow rate on morphological properties of the Ti-Al-N films.

Temperature (°C)	Nitrogen Flow Rate (sccm)	Thickness (μm)	RMS (nm)
200	20	1.64	6.5
	40	1.35	2.2
	60	0.81	1.0
500	20	1.12	8.2
	40	0.62	13.0
	60	0.68	13.9

For the samples prepared at 500 °C (Figure 2d–f), a completely different evolution was found. While for a low nitrogen flux, a network-like surface structure consisting of non-separable grains is present, at higher fluxes, larger, well-separated features appear. In contrast to the low temperature, the coatings have more surface defects, accompanied by increasing surface roughness. Thus, the process temperature has major influence on the growth and surface roughness (an average quantity) of the coating, whereas nitrogen flux determines the shape of single grains (a local quantity). These findings may be caused by different growth rates and nucleation properties during deposition. Furthermore, the thicknesses for both series decrease with higher nitrogen content, because the densities of gas molecules increase with rising nitrogen flow rate, which leads to more collisions and reduced thickness of the coatings [26]. Poisoning of the target by nitrogen can be a reason for this change, too [27].

3.2. XPS

The surface of the coatings was analyzed by XPS before an ion bombardment cleaning process, in order to understand the chemical bonding state of the surface. The Ar⁺ etching rate was about

2 Å/min. The initial surfaces were strongly contaminated and oxidized in all cases. After Ar⁺ etching, a substantial decrease of carbon content and higher intensity of Al2p, N1s and Ti2p lines due to surface cleaning were noticed. This behavior was typical for all samples.

Thus, all samples were analyzed after 30 min argon etching to remove the top contaminant layer. Figure 3a–f shows typical high resolution XPS-spectra Ti2p core levels of coatings prepared at different nitrogen flow rates and temperatures, respectively. Titanium is represented by three main states, which correspond to (Ti,Al)N (455.6–455.7 eV, black), TiON (457.3–457.7 eV, blue) and TiO₂ (459.0–459.4 eV, red) [28–30]. The titanium states do not correlate with the nitrogen content as well as the preparation temperature of the samples. No significant differences in binding energy between the analysed samples was found.

Aluminum was represented by two states with binding energies of 74.1–74.2 eV and 74.9–75.4 eV (Figure 4a–f), which correspond to oxynitride and nitride AlN (a standard binding energy of 73.5–73.8 eV) [31,32] and oxide Al₂O₃ [33,34]. A correlation of aluminum oxide concentration with the nitrogen content was found in the 200 °C series. Increasing N content leads to an increase of the oxynitride (nitride) fraction and decrease of the Al₂O₃ fraction. No correlation of the Al state with the nitrogen content in the 500 °C series was observed; the corresponding spectra are almost the same. This means that at high temperature treatment, the equilibrium surface composition is reached independently of the initial aluminum content.

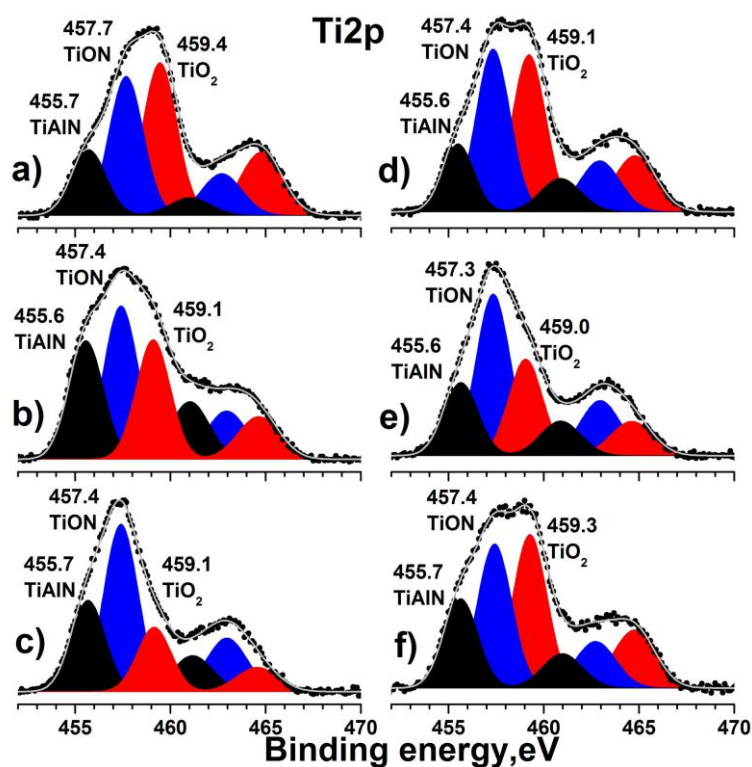


Figure 3. Ti2p XP-spectra obtained for Ti-Al-N films (a) 200 °C, 20 sccm; (b) 200 °C, 40 sccm; (c) 200 °C, 60 sccm; (d) 500 °C, 20 sccm; (e) 500 °C, 40 sccm and (f) 500 °C, 60 sccm after Ar⁺ ion etching.

The nitrogen valence state represented mainly by the peak at 396.8–396.9 eV is corresponding to nitride as well as oxynitride (396.6 eV) (Figure 5a–f) due to the close position of N1s for pure TiN (396.8 eV) and AlN (397.3 eV), respectively [29,31,35]; these states are not resolved on the binding energy. The peak centered at approximately 398.5 eV may be attributed to the shake-up satellite [29]. An increase in N1s intensity with increasing nitrogen amount can be observed for coatings deposited at 200 °C, whereas no correlation was observed for coatings at 500 °C. This is similar to the aluminum

behavior and could be related with reaching the equilibrium surface composition, regardless of initial elements' concentrations.

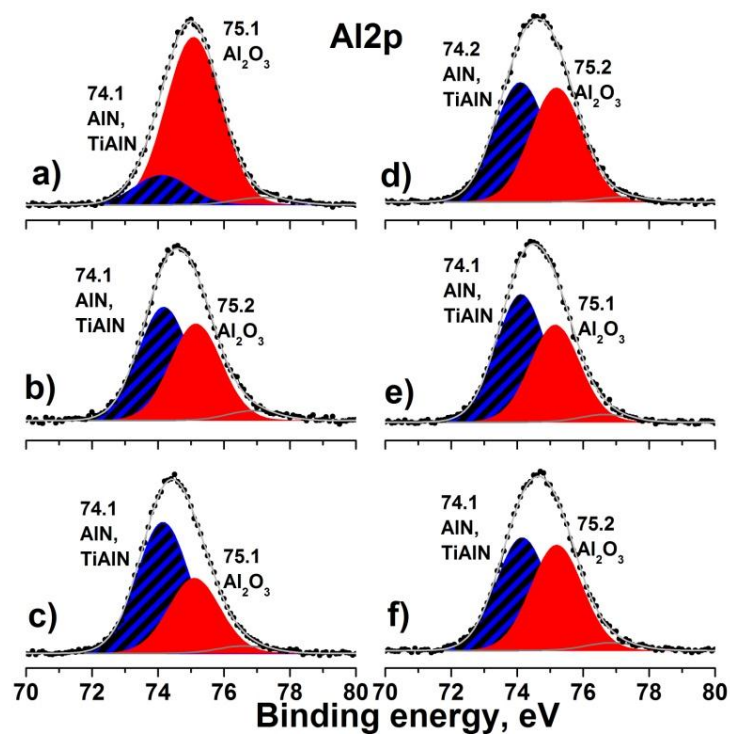


Figure 4. Al₂p XP-spectra obtained for Ti-Al-N films (a) 200 °C, 20 sccm; (b) 200 °C, 40 sccm; (c) 200 °C, 60 sccm; (d) 500 °C, 20 sccm; (e) 500 °C, 40 sccm and (f) 500 °C, 60 sccm after Ar⁺ ion etching.

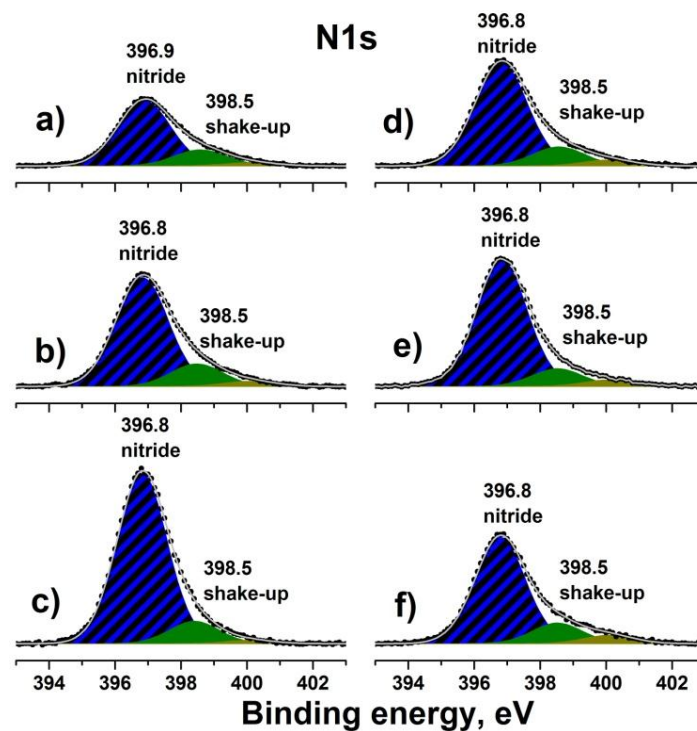


Figure 5. N₁s XP-spectra obtained for Ti-Al-N films (a) 200 °C, 20 sccm; (b) 200 °C, 40 sccm; (c) 200 °C, 60 sccm, (d) 500 °C, 20 sccm, (e) 500 °C, 40 sccm and (f) 500 °C, 60 sccm after Ar⁺ ion etching.

3.3. Nanoindentation

Figure 6 shows the relationship between hardness and elastic modulus as a function of nitrogen content at two deposition temperatures. At 500 °C, the coating deposited with 20 sccm has the highest hardness and lowest modulus (30.5 GPa and 215 GPa, respectively). In comparison to this, at 200 °C, hardness first decreases and then rises with increasing nitrogen flow rate. Nanoindentation results correlate with the WDS analysis, because mechanical properties increase with Al content and reach a maximum value at 43–44 at. % of Al, close to the results reported by other groups [25,36]. Moreover, the deterioration of mechanical properties with the increase in nitrogen content can be related to the achievement of saturation level due to higher nitrogen pressure leading to excess of nitrogen in the interstitial sites [37]. This excess of nitrogen could lead to an increase in grain size, a change in crystallographic orientations, and affect film density, lattice parameter and the stoichiometry of the coatings [38,39]. A reason for high standard deviations is the high surface roughness of the coating, which influences the indentation depth during the nanoindentation measurements.

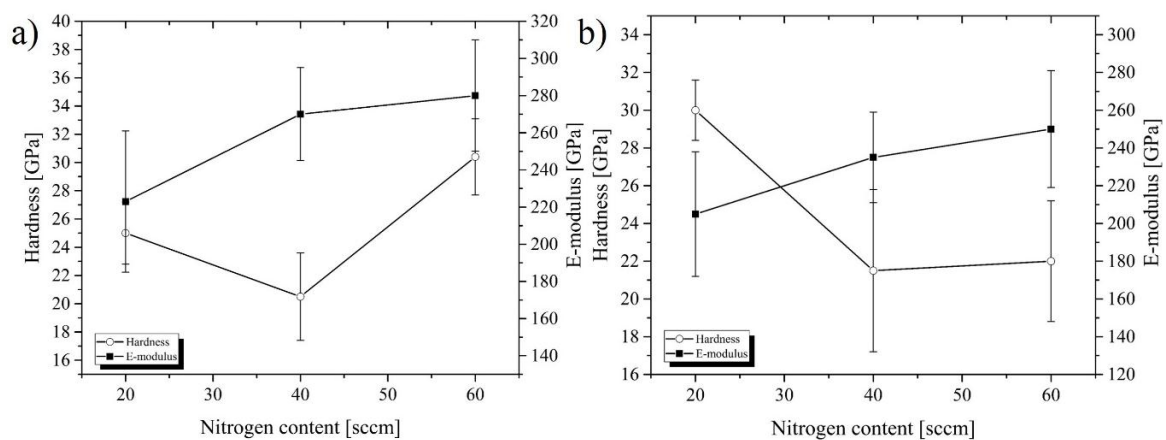


Figure 6. Influence of the nitrogen flow rate on mechanical properties of the Ti-Al-N coatings at: (a) 200 °C and (b) 500 °C.

3.4. Cylindrical Turning Experiments

Ti-Al-N coating deposited at 500 °C with N₂ flow of 20 sccm was chosen for the deposition on the WC cutting tool due to its high hardness and low modulus. The result of machining the hardened X210CrW12 steel is presented in Figure 7. A quasi-constant flank wear can be seen until a machining volume of 23,500 mm³, followed by rapid material removal until the criterion was fulfilled. In comparison to the results reported by Uhlmann et al. [24] (Figure 7), the Ti-Al-N coating in the current study shows virtually twice higher machining volume. An alternative method to the direct current magnetron sputtering (DCMS) is the high pulsed power magnetron sputtering (HPPMS), which is believed to provide better mechanical properties and high adhesion between the coating and the substrate [23]. Industry has been using HPPMS as a coating method during the last years, but not much information can be found in the literature regarding the wear properties of these coatings. Hence, investigations on the wear behaviour of HPPMS deposited Ti-Al-N coatings will be made in the future.

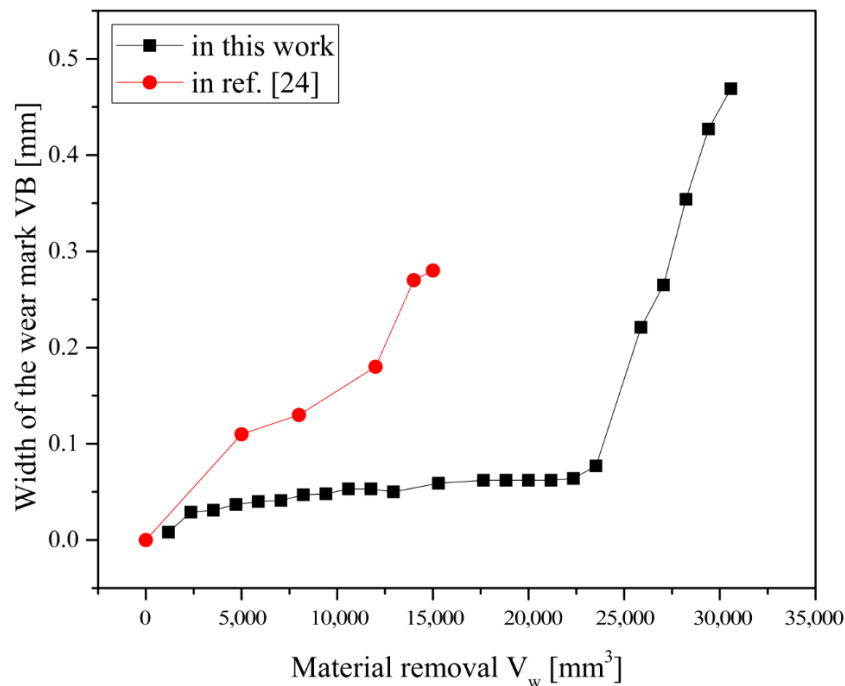


Figure 7. Development of wear for the turning test of WC with the Ti-Al-N coating.

4. Conclusions

Ti-Al-N coatings were prepared at different temperatures and nitrogen flow rates using a reactive sputter deposition process. The process parameters were optimized to achieve good mechanical properties of the films. AFM results reveal that the process temperature has major influence on growth and surface roughness of the films, whereas the nitrogen flow rate affects the shape of the grains. XPS results reveal that the bonding structure of all coatings exhibited the (Ti,Al)N phase. The nanoindentation data indicated that the coating deposited at 500 °C and 20 sccm exhibited the best mechanical properties. Moreover, mechanical properties depend on Al content within the coating. A coating with these parameters was used for deposition onto WC cutting tools, which showed low material removal rate during cylindrical turning experiments.

Acknowledgments: The authors are thankful to Bartek Stawiszynski (Technical University Berlin, IWF) for cylindrical turning experiments and for the scientific discussions.

Author Contributions: Aleksei Obrosof carried out the deposition process with the help of Muhammad Naveed. Aleksei Obrosof analyzed the results and prepared the paper with the help of Alex A. Volinsky. Marcus Ratzke provided AFM results. Roman Gulyaev carried out XPS analysis and described the results. Sebastian Bolz provided SEM and WDX investigations. Sabine Weiß revised the manuscript and directed the work.

Conflicts of Interest: The authors declare no conflict of interest.

References

1. Münz, W.D. Titanium aluminum nitride films: A new alternative to tin coatings. *J. Vac. Sci. Technol. A* **1986**, *4*, 2717–2725. [[CrossRef](#)]
2. Knotek, O.; Münz, W.D.; Leyendecker, T. Industrial deposition of binary, ternary, and quaternary nitrides of titanium, zirconium, and aluminum. *J. Vac. Sci. Technol. A* **1987**, *5*, 2173–2179. [[CrossRef](#)]
3. Barshilia, H.C.; Prakash, M.S.; Jain, A.; Rajam, K.S. Structure, hardness and thermal stability of TiAlN and nanolayered TiAlN/CrN multilayer films. *Vacuum* **2005**, *77*, 169–179. [[CrossRef](#)]
4. Shieh, J.; Hon, M.H. Nanostructure and hardness of titanium aluminum nitride prepared by plasma enhanced chemical vapor deposition. *Thin Solid Films* **2001**, *391*, 101–108. [[CrossRef](#)]

5. Bressan, J.D.; Hesse, R.; Silva, E.M., Jr. Abrasive wear behavior of high speed steel and hard metal coated with TiAlN and TiCN. *Wear* **2001**, *250*, 561–568. [[CrossRef](#)]
6. Yang, Q.; Seo, D.Y.; Zhao, L.R.; Zeng, X.T. Erosion resistance performance of magnetron sputtering deposited TiAlN coatings. *Surf. Coat. Technol.* **2004**, *188–189*, 168–173. [[CrossRef](#)]
7. Kimura, A.; Hasegawa, H.; Yamada, K.; Suzuki, T. Effects of Al content on hardness, lattice parameter and microstructure of $Ti_{1-x}Al_xN$ films. *Surf. Coat. Technol.* **1999**, *120–121*, 438–441. [[CrossRef](#)]
8. Pfeiler, M.; Fontalvo, G.A.; Wagner, J.; Kutschej, K.; Penoy, M.; Michotte, C.; Mitterer, C.; Kathrein, M. Arc evaporation of Ti–Al–Ta–N coatings: The effect of bias voltage and Ta on high-temperature tribological properties. *Tribol. Lett.* **2008**, *30*, 91–97. [[CrossRef](#)]
9. Suzuki, T.; Huang, D.; Ikuhara, Y. Microstructures and grain boundaries of (Ti,Al)N films. *Surf. Coat. Technol.* **1998**, *107*, 41–47. [[CrossRef](#)]
10. Sergevnin, V.S.; Blinkov, I.V.; Belov, D.S.; Volkhonskii, A.O.; Skryleva, E.A.; Chernogor, A.V. Phase formation in the Ti–Al–Mo–N system during the growth of adaptive wear-resistant coatings by arc pvd. *Inorg. Mater.* **2016**, *52*, 735–742. [[CrossRef](#)]
11. Shugurov, A.R.; Akulinkin, A.A.; Panin, A.V.; Perevalova, O.B.; Sergeev, V.P. Structural modification of tialn coatings by preliminary Ti ion bombardment of a steel substrate. *Tech. Phys.* **2016**, *61*, 409–415. [[CrossRef](#)]
12. PalDey, S.; Deevi, S.C. Single layer and multilayer wear resistant coatings of (Ti,Al)N: A review. *Mater. Sci. Eng. A* **2003**, *342*, 58–79. [[CrossRef](#)]
13. Musil, J.; Hrubý, H. Superhard nanocomposite $Ti_{1-x}Al_xN$ films prepared by magnetron sputtering. *Thin Solid Films* **2000**, *365*, 104–109. [[CrossRef](#)]
14. Anikin, V.N.; Blinkov, I.V.; Volkhonskii, A.O.; Sobolev, N.A.; Tsareva, S.G.; Kratokhvil, R.V.; Frolov, A.E. Ion-plasma Ti–Al–N coatings on a cutting hard-alloy tool operating under conditions of constant and alternating-sign loads. *Russ. J. Non-Ferr. Met.* **2009**, *50*, 424–431. [[CrossRef](#)]
15. Kimura, A.; Murakami, T.; Yamada, K.; Suzuki, T. Hot-pressed Ti–Al targets for synthesizing $Ti_{1-x}Al_xN$ films by the arc ion plating method. *Thin Solid Films* **2001**, *382*, 101–105. [[CrossRef](#)]
16. Stepanov, I.B.; Ryabchikov, A.I.; Ananin, P.S.; Bumagina, A.I.; Shevelev, A.E.; Shulepov, I.A.; Sivin, D.O. Investigation of filtered vacuum arc plasma application for tialn and TiSiB coatings deposition using ion beam and plasma material processing. *Surf. Coat. Technol.* **2016**, *296*, 20–25. [[CrossRef](#)]
17. Quesada, F.; Mariño, A.; Restrepo, E. TiAlN coatings deposited by r.f. Magnetron sputtering on previously treated ASTM A36 steel. *Surf. Coat. Technol.* **2006**, *201*, 2925–2929. [[CrossRef](#)]
18. Oliveira, J.C.; Manaia, A.; Cavaleiro, A. Hard amorphous Ti–Al–N coatings deposited by sputtering. *Thin Solid Films* **2008**, *516*, 5032–5038. [[CrossRef](#)]
19. Kutschej, K.; Mayrhofer, P.H.; Kathrein, M.; Polcik, P.; Tessadri, R.; Mitterer, C. Structure, mechanical and tribological properties of sputtered $Ti_{1-x}Al_xN$ coatings with $0.5 \leq x \leq 0.75$. *Surf. Coat. Technol.* **2005**, *200*, 2358–2365. [[CrossRef](#)]
20. Gulyaev, R.V.; Koscheev, S.V.; Malykhin, S.E. An algorithm for removing charging effects from X-ray photoelectron spectra of nanoscaled non-conductive materials. *J. Electron Spectrosc. Related Phenom.* **2015**, *202*, 89–101. [[CrossRef](#)]
21. Oliver, W.C.; Pharr, G.M. An improved technique for determining hardness and elastic modulus using load and displacement sensing indentation experiments. *J. Mater. Res.* **1992**, *7*, 1564–1583. [[CrossRef](#)]
22. Obrosov, A.; Naveed, M.; Volinsky, A.A.; Weiß, S. Substrate frequency effects on Cr_xN coatings deposited by DC magnetron sputtering. *J. Mater. Eng. Perform.* **2017**, *26*, 366–373. [[CrossRef](#)]
23. Uhlmann, E.; Stawiszynski, B.; Leyens, C.; Heinze, S.; Sammler, F. Hard turning of hot work and cold work steels with hipims and dcms TiAlN coated carbide inserts. *Proced. CIRP* **2016**, *46*, 591–594. [[CrossRef](#)]
24. Uhlmann, E.; Stawiszynski, B.; Leyens, C.; Heinze, S. HiPIMS coated carbides with high adhesive strength for hard machining. In Proceedings of the 11th International Conference on High Speed Machining 2014, Prag, Czech Republic, 11–12 September 2014.
25. Shum, P.W.; Zhou, Z.F.; Li, K.Y.; Shen, Y.G. XPS, AFM and nanoindentation studies of $Ti_{1-x}Al_xN$ films synthesized by reactive unbalanced magnetron sputtering. *Mater. Sci. Eng. B* **2003**, *100*, 204–213. [[CrossRef](#)]
26. Li, D.; Chen, J.; Zou, C.; Ma, J.; Li, P.; Li, Y. Effects of Al concentrations on the microstructure and mechanical properties of Ti–Al–N films deposited by RF-ICPIS enhanced magnetron sputtering. *J. Alloy. Compd.* **2014**, *609*, 239–243. [[CrossRef](#)]

27. Zhou, W.; Liang, J.; Zhang, F.; Mu, J.; Zhao, H. A comparative research on TiAlN coatings reactively sputtered from powder and from smelting tial targets at various nitrogen flow rates. *Appl. Surf. Sci.* **2014**, *313*, 10–18. [[CrossRef](#)]
28. Tezuka, Y.; Shin, S.; Ishii, T.; Ejima, T.; Suzuki, S.; Sato, S. Photoemission and bremsstrahlung isochromat spectroscopy studies of TiO₂ (rutile) and SrTiO₃. *J. Phys. Soc. Jpn.* **1994**, *63*, 347–357. [[CrossRef](#)]
29. Prieto, P.; Kirby, R.E. X-ray photoelectron spectroscopy study of the difference between reactively evaporated and direct sputter-deposited TiN films and their oxidation properties. *J. Vac. Sci. Technol. A* **1995**, *13*, 2819–2826. [[CrossRef](#)]
30. Hopfengärtner, G.; Borgmann, D.; Rademacher, I.; Wedler, G.; Hums, E.; Spitznagel, G.W. XPS studies of oxidic model catalysts: Internal standards and oxidation numbers. *J. Electron Spectrosc. Relat. Phenom.* **1993**, *63*, 91–116. [[CrossRef](#)]
31. Bertóti, I. Characterization of nitride coatings by XPS. *Surf. Coat. Technol.* **2002**, *151–152*, 194–203. [[CrossRef](#)]
32. Dejun, K.; Haoyuan, G. Friction-wear behaviors of cathodic arc ion plating AlTiN coatings at high temperatures. *Tribol. Int.* **2015**, *88*, 31–39. [[CrossRef](#)]
33. Rizzo, A.; Mirengi, L.; Massaro, M.; Galietti, U.; Capodici, L.; Terzi, R.; Tapfer, L.; Valerini, D. Improved properties of tialn coatings through the multilayer structure. *Surf. Coat. Technol.* **2013**, *235*, 475–483. [[CrossRef](#)]
34. Motamedi, P.; Cadien, K. XPS analysis of AlN thin films deposited by plasma enhanced atomic layer deposition. *Appl. Surf. Sci.* **2014**, *315*, 104–109. [[CrossRef](#)]
35. Cai, F.; Zhang, S.; Li, J.; Chen, Z.; Li, M.; Wang, L. Effect of nitrogen partial pressure on Al–Ti–N films deposited by arc ion plating. *Appl. Surf. Sci.* **2011**, *258*, 1819–1825. [[CrossRef](#)]
36. Zhou, M.; Makino, Y.; Nose, M.; Nogi, K. Phase transition and properties of Ti–Al–N thin films prepared by r.f.-plasma assisted magnetron sputtering. *Thin Solid Films* **1999**, *339*, 203–208. [[CrossRef](#)]
37. Garfunkel, E.; Gusev, E.; Vul', A. *Fundamental Aspects of Ultrathin Dielectrics on Si-Based Devices*; Springer Netherlands: Dordrecht, The Netherlands, 2012.
38. Yeung, W.Y.; Dub, S.N.; Wuhler, R.; Milman, Y.V. A nanoindentation study of magnetron co-sputtered nanocrystalline ternary nitride coatings. *Sci. Sinter.* **2006**, *38*, 212–214. [[CrossRef](#)]
39. Patsalas, P.; Charitidis, C.; Logothetidis, S. The effect of substrate temperature and biasing on the mechanical properties and structure of sputtered titanium nitride thin films. *Surf. Coat. Technol.* **2000**, *125*, 335–340. [[CrossRef](#)]



© 2017 by the authors; licensee MDPI, Basel, Switzerland. This article is an open access article distributed under the terms and conditions of the Creative Commons Attribution (CC BY) license (<http://creativecommons.org/licenses/by/4.0/>).